Closing report: NKFI-OTKA grant K116602

Introduction

Small RNA (sRNA) mediated RNA interference (RNAi) is a widespread regulatory mechanism playing role in diverse biological processes in most eukaryotic organisms. Micro RNAs (miRNAs), a subclass of sRNAs, are predominantly responsible for controlling endogenous gene expression and are major regulators of plant growth, development, biotic-abiotic stress responses and perception of light or nutrition fluctuations. During the biogenesis of miRNAs, a genome-encoded RNA (primary miRNA (pri-miRNA)) with specific stem-loop secondary RNA structure is subjected to subsequent cleavages producing 21-24 nucleotide (nt) long miRNA duplexes. The stem-loops of plant pri-miRNAs exhibit extreme variability in length and structure compared to animal counterparts. In plants, miRNA precursors (pre-miRNAs) are typically excised initially from pri-miRNA transcripts by the action of DICER-LIKE1 (DCL1) with a cleavage event near the base of the stem. The next DCL1 cleavage occurs in 21-24 nucleotide distance from the end of the stem resulting in a miRNA duplex. The generated miRNA intermediate duplexes consist of a guide (miRNA) and a passenger (miRNA*) strand with 2-nt 3′ overhang and a 5′ phosphate at each strand. The methylated miRNA/miRNA∗ duplexes, according to the previous model, were thought to be exported to the cytoplasm by the animal Exportin 5 (EXPO5) homologous protein HASTY (HST). During the assembly of RNA-induced Silencing Complex (RISC), one strand of the miRNA/miRNA* duplex (the guide miRNA strand) is loaded onto ARGONAUTE1 (AGO1) protein and the other strand (star strand, miRNA*) is ejected and degraded. AGO1 is the major effector protein for miRNAs among the ten *Arabidopsis* encoded AGO proteins which are specialized for various RNAi pathways but often display functional redundancies. There are also structural elements on miRNA/miRNA* duplexes determining the association of the miRNA with the specific AGO proteins. Expression of AGO1 protein itself is also under the control of RNAi regulatory process through the action of miR168. Furthermore, *AGO1* and *MIR168* gene expressions are regulated co-transcriptionally. Regulation of AGO1 level also involves the coordinated action of *AGO1*-derived small interfering (si)RNAs. The existence of two miR168 producing primary transcripts (*MIR168a* and *MIR168b)* with both distinct and overlapping functions gives an additional layer to the control of AGO1. The central role of AGO1 in the action of miRNA pathway is reflected by the fact that *ago1* null mutations are lethal and hypomorfic *ago1* mutants show severe phenotypes. Moreover, over-accumulation of AGO1 also induces disturbances in miRNA levels and extremely drastic phenotypic alterations. These data indicate that fine-tuning of AGO1 homeostasis is crucial and consequently involves many regulation levels.

The objectives of the grant

1. Elaboration and utilization a technology suitable for identification of RISC bound biologically active smRNAs by NGS in Arabidopsis and crop plants.

2. Investigation of molecular mechanism of miR168 mediated regulation of AGO1 in Arabidopsis.

3. Establishment a gain of function mutant screen for identification influencing the activity of RNA interference.

Results

1.Elaboration and utilization a technology suitable for identification of RISC bound biologically active smRNAs by NGS in Arabidopsis and crop plants.

Using gel-filtration assays we identified three pools of sRNAs at a genome-wide level based on the molecular size-dependent mobility of nucleoprotein complexes. High-throughput sequencing (HTS) analyses of these pools revealed that their molecular composition is markedly different confirming that they are distinct biological entities. We show that canonical miRNAs predominantly associate with a high molecular weight (HMW) RISC which co-migrates with AGO1. By providing HTS data we show that the 24-nt siRNAs are mainly associated with a low molecular weight (LMW) RISC co-migrating with AGO4. More intriguingly, we identified a large pool of protein-unbound sRNAs containing 2'-*O*-methylated mature and star sequences of annotated miRNAs potentially in a double-stranded form and also unloaded 23- and 24-nt siRNAs. We show that miRNAs differ in their RISC-loading efficiencies indicated by their different distribution between the AGO-bound and -unbound pools. Moreover, we demonstrate that the RISC-loading efficiency of some miRNAs can be different between tissues. This can be partly attributed to the different level of AGO proteins because the loading level of miRNAs can be enhanced by overexpressing AGO proteins. We also show in transient and stable transgenic expression systems that the RISC-loading efficiencies of distinct miRNAs are predominantly controlled by their diverse precursor RNAs. Based on our findings we suggest a model for a new regulatory mechanism which determines the biological activity of miRNAs by controlling their RISC loading efficiencies through the action of diverse precursor RNAs. We also think that our results can be useful from a practical point of view for scientists designing artificial (a)miRNAs (precursor backbone selection, modification for optimal results, enhancing or reducing amiRNA activity).

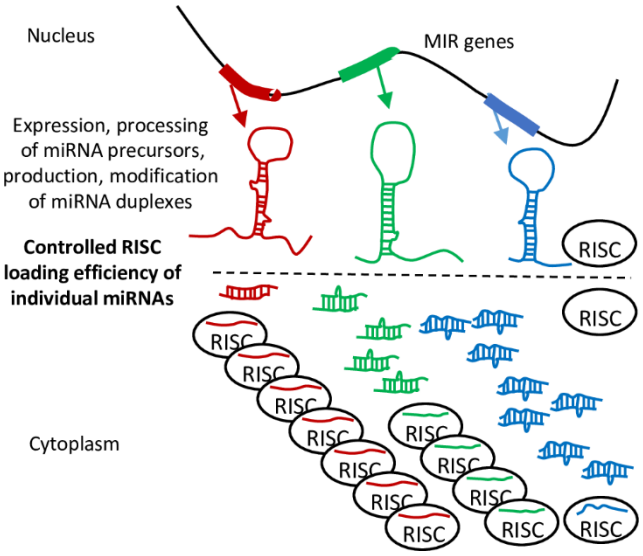

Schematic representation of the proposed model. Genome-encoded MIR genes (red, green and blue boxes) are transcribed to various, extremely diverse miRNA precursors (hairpin structures) according to the regulated activities of their promoters. The different miRNA precursors are processed to miRNA intermediate duplexes containing the mature and passenger (*) miRNA strands. These miRNAs undergo methylation at the 3' nucleotide. The next step is the selective loading of the mature

miRNA stands (red, green and blue curved lines) into the executor complexes, the AGO1 containing RISCs (black circles), while the miRNA* strands are eliminated. However, here, a newly identified regulatory mechanism, likely controlled by information carried on the diverse miRNA precursors, determines the RISC-loading efficiencies of various miRNAs sorting only a subset of the produced miRNAs into the biologically active RISCs. The superfluous miRNA populations accumulate in the cytoplasm as protein-unbound pool very likely as miRNA:miRNA* duplexes. Due to this regulation, miRNAs have high (red), intermediate (green), or low (blue) RISC-loading capacities in the given cellular environment. The availability of unloaded RISCs can influence loading properties of miRNAs suggesting that excess of sRNA population compete for limiting empty RISCs. The place of RISC-loading is not known, it can be either in the cytoplasm or nucleus (empty RISC circles). It is also unknown whether the cytoplasmic pool of protein-unbound miRNAs can be redirected to RISCs or they represent biologically inactive products. Altogether, this model suggests that the production rate of certain miRNAs is not the only factor which determines their biological activity. A highly controlled post-production regulatory mechanism can determine the biologically active portion of the produced miRNA population by adjusting their RISC-loading efficiencies in the given cellular environment.

These results have been published in "Dalmadi Á, Gyula P, Bálint J, Szittya G, Havelda Z. (2019) **AGO-unbound cytosolic pool of mature miRNAs in plant cells reveals a novel regulatory step at AGO1 loading. Nucleic Acids Res.** 2019 Oct 10;47(18):9803-9817. (IF 11.1) Scimago D1.

To adapt this technology for economically important plant, first we established the crude extract and sRNA HTS sequencing protocols for pepper (*Capsicum annuum*). To get high-resolution spatiotemporal information about dynamic sRNA expression pattern associated with the expansion phase of the pepper fruit development, we dissected the fruit. We collected flesh, seed, and placenta samples at 28 and 40 days after anthesis (DAA), and quantified their small RNA populations by high-throughput sequencing. Using the gained datasets, we generated the comparative tissue-specific differential expression profiles of the conserved, the already described, and the newly predicted pepper-specific miRNAs. We found that differential expression activity of miRNAs is intriguingly high at 40 DAA and especially the expansion of flesh is associated with profound changes in the miRNA expression profile. The pronounced role of miRNA-mediated regulation in flesh development was also reflected by the high level of AGO1 protein present in flesh samples. Moreover, the analyses of non-miRNA-like sRNAs revealed an ample of pepper-specific hetsiRNAs and phasiRNAs playing a role mainly in the development of the seed and the placenta.

These results have been published in: Taller D, Bálint J, Gyula P, Nagy T, Barta E, Baksa I, Szittya G, Taller J, Havelda Z. (2018) **Expansion of Capsicum annum fruit is linked to dynamic tissue-specific differential expression of miRNA and siRNA profiles. PLoS One**. 2018 Jul 25;13(7) (IF 2.8) Scimago Q1.

Next we used the dissected pepper tissue samples (flesh, seed and placenta) and used them in gel-filtartion experiments to identify sRNAs in different fractions. 24 small RNA libraries were produced and sequenced on Illumina platform. The received small RNA data set has been trimmed and the basic bioinformatic analyses has been carried out. The size distribution of sRNAs showed similar results to that of the Arabidopsis data indicating that our results biologically relevant.

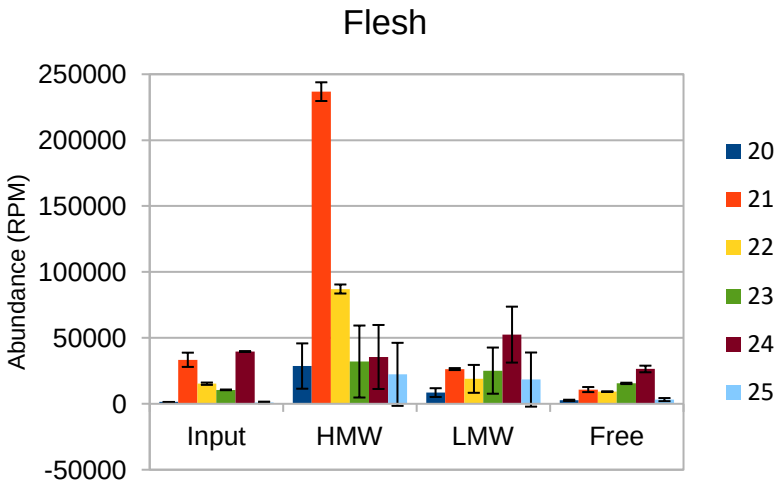

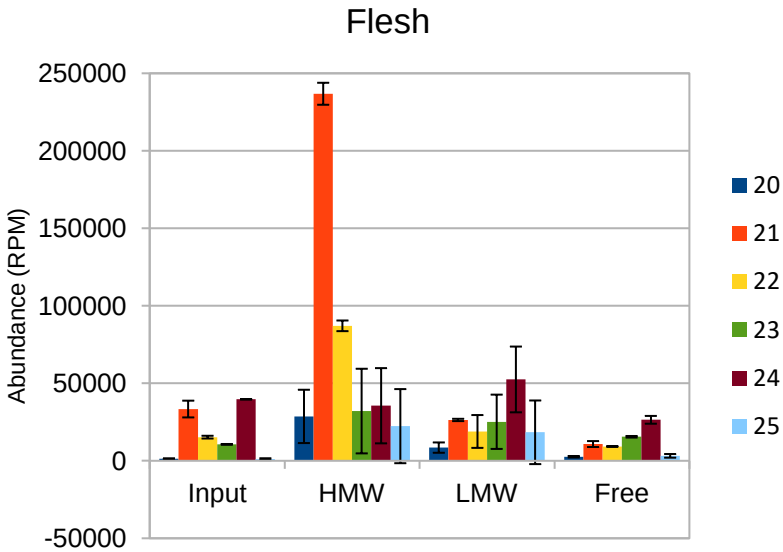

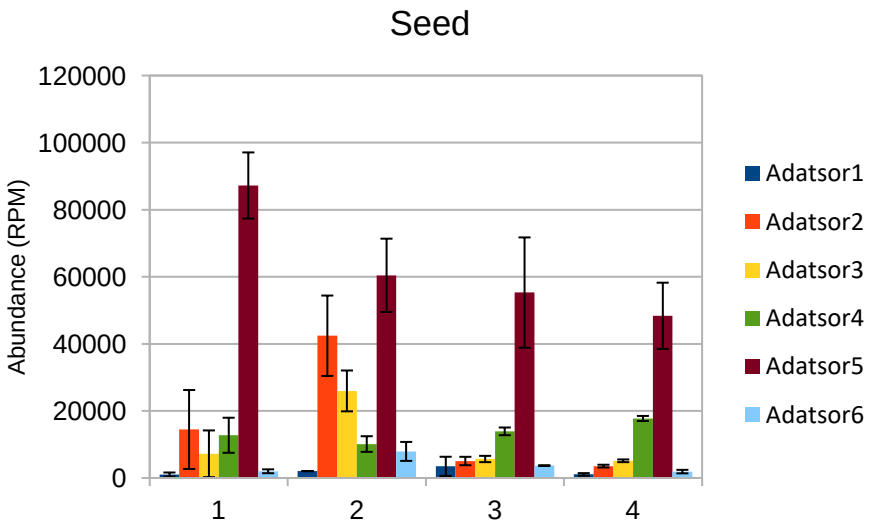

Size distribution (20-25 nt) of pepper specific sRNAs in different tissue types relative to the input total RNA sRNA content. HMW (High Molecular Weight RISC), LMW (Low Molecular Weight RISC) and free, protein unbound sRNAs.

Using the LMW data set, which contains the AGO1 loaded biologically active sRNAs, we were able to identify potentially new, pepper specific miRNAs. The proper expression of these new pepper specific has been validated by small RNA Northern blot.

The further analyses of the data and the wet laboratory experiments are currently running in the laboratory.

2.Investigation of molecular mechanism of miR168 mediated regulation of AGO1 in Arabidopsis.

Over-expression of miR168 from *ath-MIR168* precursors induces limited AGO1 down-regulation.

First, we investigated the AGO1 controlling efficiency of miR168, over-produced from the wild type *A. thaliana MIR168a* precursor. To test AGO1 controlling activity of miR168 in transient assays, a sensor construct was built by fusing the 558 base pair long 5' section of *ath-AGO1* gene containing miR168 target site in frame to 5' end of GFP under the control of 35S promoter (*AGO1-sensor*; Fig. 1A). 35S::*MIR168a* binary construct (*MIR168a*) was expressed transiently in *Nicotiana benthamiana* leaves by *Agrobacterium* infiltration in the presence of *AGO1-sensor.* To eliminate siRNA mediated transgene induced RNAi, viral p14 silencing suppressor construct was added to every *Agrobacterium* suspension in an equal proportion. Robust miR168 over-expression resulted in only a moderate decrease in GFP signal of *AGO1-sensor* compared to control infiltration with empty vector (Fig. 1B). Accumulation of *AGO1-sensor* was tested by Western blots using an *A. thaliana* specific AGO1 antibody not recognizing the *N. benthamiana* AGO1. The *AGO1-sensor* showed also moderate down-regulation. To further investigate the regulatory efficiency of miR168 on AGO1 accumulation we produced transgenic *A. thaliana* (Columbia) plants over-expressing both wild type *MIR168a* and *MIR168b*. In accordance with a previous work, transgenic over-expression of *MIR168a* caused only minor changes in the phenotype as we observed only slightly serrated rosette leaves and delayed flowering in transgenic lines (Fig. 1C). The severity of the phenotypes correlated with miR168 accumulation levels and the overall look and fertility of mature plants resembled to the wild type ones. Western blot analyses of *MIR168a* over-expressing transgenic lines also detected only a moderate down-regulation of AGO1 level compared to wild type plant (Fig. 1C). Similarly to previous results, we detected slightly decreased accumulation of miR159 in parallel with the reduced AGO1 level. Over-expression of *MIR168b* induced the same mild phenotypic alterations as observed for *MIR168a* and also associated with moderate AGO1 protein down-regulation in young leaves. Since *35S::MIR168a* and *35S::MIR168b* transgenic plants exhibited similar phenotypes and AGO1 down-regulation properties, only *35S::MIR168a* lines were used in following experiments. To investigate the loading efficiency of miR168 into AGO1-RISC in both, wild type and *MIR168a* precursor over-producing plants size separation gel-filtration assay was used. Crude extracts of young leaves were loaded onto size-separating column and the collected fractions were analysed for their miRNA and AGO1

protein content. In line with our previous data, miR159 was present predominantly in high molecular weight (HMW) AGO1-RISC containing complexes. In contrast, miR168 accumulated mainly in protein unbound form and only the minority of miR168 was loaded into HMW AGO1-RISC (Fig. 1D). Similarly, as was described previously the elevated miR168 level resulted only in a moderate increase in HMW AGO1-RISC loading of miR168 (Fig. 1D). This observation indicates that the massive excess of miR168 matured from over-produced wild type *MIR168a* precursor is not able to incorporate into AGO1-RISC efficiently. This restricted loading efficiency of miR168 resulted only in a moderately reduced AGO1 protein level. The majority of the produced miR168 accumulated in fractions representing protein unbound miRNAs. This phenomenon is characteristic of miR168 since transient or transgenic over-expression of miR159 and miR171 results in almost total or very efficient loading of HMW AGO1-RISC, respectively. In *MIR168a* over-expressing plants, miR159 preserved its well-loading feature (Fig. 1D). This observation confirms that not the unavailability of free, unloaded AGO1 proteins limits the incorporation of miR168 into AGO1-RISC. Altogether, the observation that *MIR168a* precursor mediated miR168 over-accumulation is not associated with enhanced AGO1-RISC loading efficiency implies the action of an equilibrium based regulatory mechanism.

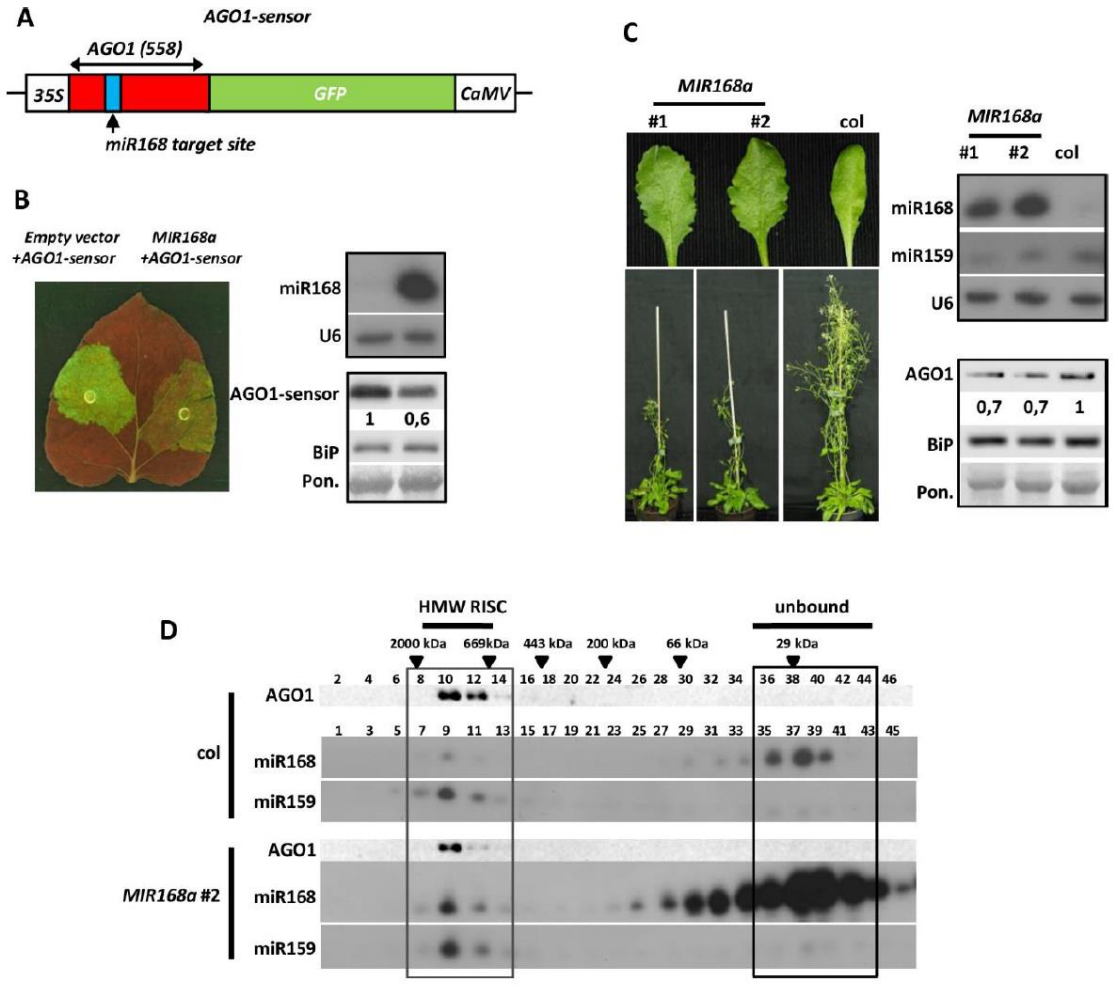

Figure 1. Over-expression of wild type *ath-pri-MIR168a* in transient and transgenic systems. (A) Schematic representation of the *AGO1-sensor* construct. AGO1-derived part of the sensor is indicated with red, miR168 target site is marked with blue rectangle. (B) Transient over-expression of *ath-pri-MIR168a* (*MIR168a* on figures) precursor in the presence of *AGO1-sensor*. Left panel shows the GFP fluorescence in leaves after co-infiltration of *AGO1-sensor* construct containing *Agrobacteria* and either empty vector (pGreen0029) or *ath-pri-MIR168a* (*MIR168a*). Right panels indicate the RNA levels of miR168 and the protein levels of the AGO1-sensor in the infiltrated patches. AGO1 part of the sensor fusion protein was detected with antibody raised against ath-AGO1. For the northern blots, U6, rRNAs, while for the western blots, BiP (Lumenal binding proteins) and Ponceau staining were used as loading controls. (C) Phenotypes of ath-pri-*MIR168a* precursor over-expressing transgenic lines. Right panels show miR168, miR159 and AGO1 levels in over-expressing and control plants. U6 and BiP, Ponceau staining were used as loading controls, respectively. (D) MiR168 distribution among gel-filtration fractions of wild type *A. thaliana* Columbia (*col*) and *ath-pri-MIR168a* over-expressing plants. High molecular weight (HMW) RISCs were detected with AGO1 western and miR159 northern blots. Even fractions were used for protein extraction, odd fractions for RNA purification. Black triangles show positions of known molecular weight markers amongst gel-filtration fractions.

Modification of miR168/miR168* duplex structure of *MIR168a* precursor can reduce AGO1 loading efficiency of miR168

According to gel filtration experiments, miRNAs processed from structurally different precursors, can be incorporated into AGO1-RISC to variant extents (Fig. 1D). Analyses of miRNA duplex structure of *MIR168* precursor RNAs originating from various species revealed a dominantly conserved mismatch position at the fourth nucleotide of miR168. To test the hypothesis that structural features have profound impact on AGO1-loading efficiency, mismatch at this position was closed by modifying the star strand creating the *MIR168-4bp* precursor (Fig. 2A). Transient over-expression of *MIR168-4bp* by agroinfiltration resulted in higher GFP signal coupled with elevated *AGO1-sensor* protein level compared to wild type *MIR168a* precursor over-expression (Fig. 2B). This observation indicates that despite of the high production rate the biological activity of *MIR168-4bp* derived miR168 species was reduced. Next, *MIR168-4bp* construct was used to generate transgenic miR168 over-expressing lines. *MIR168-4bp* and wild type *MIR168a* over-expressing lines having comparable miR168 content were selected and their phenotype and AGO1 content were analysed. The selected *MIR168-4bp* line showed less delay in flowering and higher AGO1 protein level than the corresponding *MIR168a* line suggesting inhibited control of AGO1 level (Fig. 2C). In gel filtration experiments *MIR168-4bp* showed reduced HMW-RISC loading efficiency relative to *MIR168a* over-expressing plants (Fig. 2D). This observation was further supported by AGO1 immuno-precipitation experiments detecting relatively decreased accumulation of miR168 derived from *MIR168-4bp* versus *MIR168a* . High-throughput sequencing (HTS) analyses of *MIR168a* or *MIR168-4bp* over-produced miR168 species in transgenic seedlings showed that they are predominantly produced in correct size and sequence. Moreover, no increase in *AGO1*-derived siRNA content can be detected by small RNA northern blot or HTS analyses. These data show that eliminating a mismatch from the miR168/miR168* duplex does not reduce the efficient production of miR168 but decreases its AGO1-RISC loading capacity.

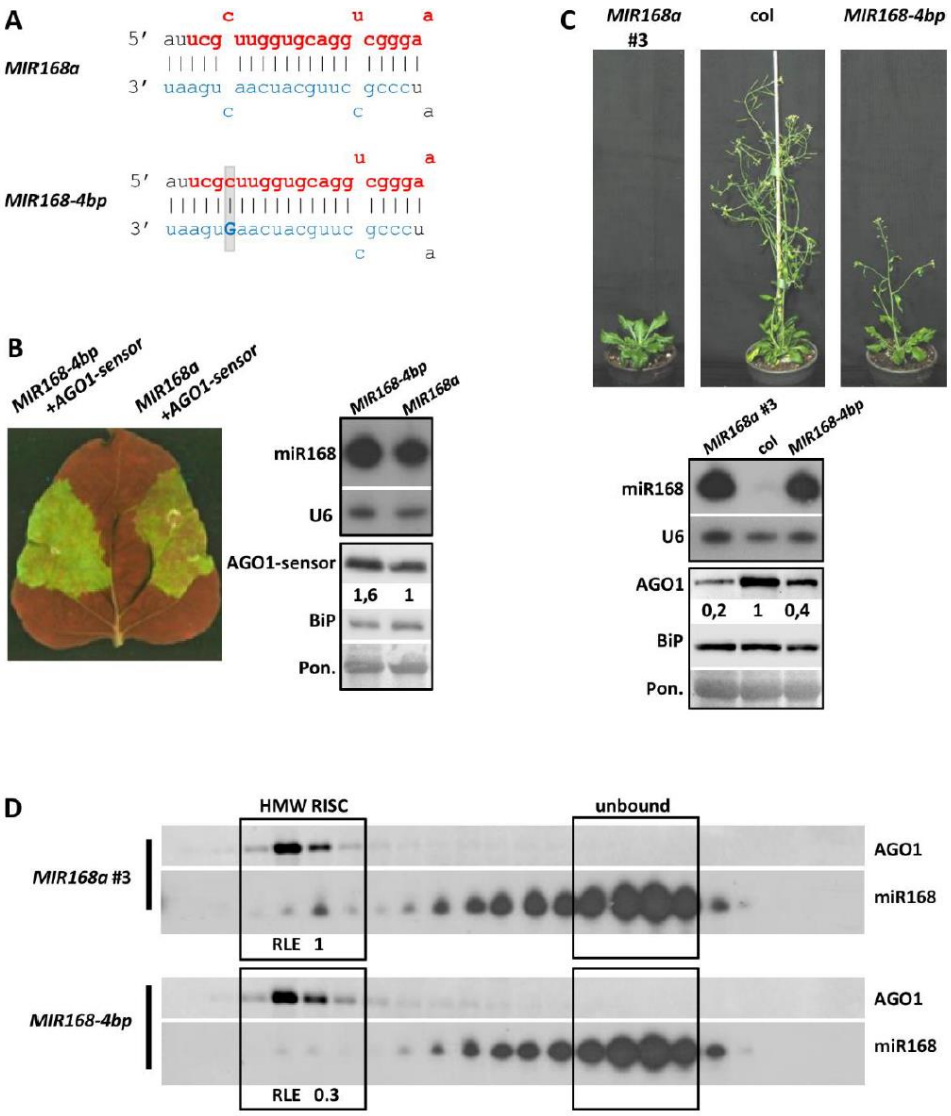

Figure 2. Effect of *MIR168a-4bp* over-expression. (A) Structure of the modified duplex region in *MIR168-4bp*. Modified nucleotide is highlighted with a bold capital letter, grey background shows structural change. (B) Transient over-expression of *MIR168-4bp* and wild type *ath-pri-MIR168a* (*MIR168a* on figures). Blots demonstrate miR168 and AGO1-sensor content in infiltrated patches of *N. benthamiana* leaves. AGO1 part of the sensor fusion protein was detected with antibody raised against ath-AGO1. For the northern blot U6, while for the western blots, BiP and Ponceau staining were used as loading controls. (C) Phenotype, miR168 and AGO1 content of a transgenic line over-expressing *MIR168-4bp* precursor and a wild type *ath-pri-MIR168a* line with comparably high (extreme) over-expression rate of miR168. (D) MiR168 distribution in gel-filtration fractions of the same lines. High molecular weight RISC is represented with AGO1. Relative loading efficiency (RLE) is calculated as described in Methods.

AGO1 loading efficiency of miR168 can be enhanced by modifying the miR168/miR168* duplex structure

To test whether AGO1 loading efficiency of miR168 can be enhanced by altering the secondary structure of the miR168/miR168* duplex, modified miRNA precursor was designed. In contrast to miR168, miR171 produced from *MIR171a* precursor in *A. thaliana*, exhibits a higher AGO1-RISC loading efficiency. Moreover, barley *hvu-MIR171* precursor produced

miR171 also shows efficient AGO1-RISC loading properties . In our previous work we have successfully used *hvu-MIR171* for producing efficient artificial miRNAs (amiRs). Next we attempted to increase the loading efficiency of miR168 into AGO1-RISC by transforming the secondary structure of miR168/miR168* duplex to mimic barley miR171/miR171*. In *hvu-MIR171* the duplex contains three mismatches at the 4th, 9th and 12th positions and the mature miRNA originates from the 3' arm of the stem-loop structure. In contrast *ath-MIR168a* has two mismatches at the 4th and 15th positions and the mature miR168 originates from 5' arm of the precursor. To mimic hvu-miR171 duplex structure mutations were introduced into the passenger strand of *ath-MIR168a* precursor to create the three mismatches in the appropriate positions, producing *MIR168-3mm* construct (Fig. 3A). The transient test of *MIR168-3mm* revealed that despite the profoundly reduced production rate of miR168, it exhibits increased capacity in down-regulating *AGO1-sensor*. Leaf patches agroinfiltrated with *MIR168-3mm* showed remarkable GFP signal reduction and low level of *AGO1-sensor* accumulation compared to *MIR168a* (Fig. 3B). Transgenic plants over-expressing *MIR168-3mm* construct showed only moderate miR168 over-expression. However, this moderate over-expression of miR168 resulted in more pronounced delay in flowering and greater AGO1 down-regulation compared to a transgenic line expressing miR168 more abundantly from the wild type *MIR168a* precursor (Fig. 3C). To test whether the enhanced activity of *MIR168-3mm* originated miR168 species is due to their altered AGO1-loading efficiency, gel filtration experiments were performed. We found that, compared to miR168 derived from *MIR168a*, miR168 produced from *MIR168_3mm* incorporates more efficiently into HMW-RISC bringing about the enhanced down-regulation of AGO1 protein (Fig. 3D). Immuno-precipitation of AGO1 from *MIR168-3mm* transgenic line also confirmed the enhanced loading efficiency of miR168 compared to the *MIR168a* transgenic line. HTS analyses of miR168 species in *MIR168-3mm* over-expressing transgenic plants showed that they are predominantly produced in correct size and sequence. Moreover, no increase in *AGO1*-derived siRNA content can be detected by small RNA northern blot or HTS analyses. These data show that reshaping the secondary structure of miR168/miR168* duplex can enhance the ability of miR168 to load into AGO1-RISC more efficiently inducing increased AGO1 protein down-regulation and phenotypic alterations.

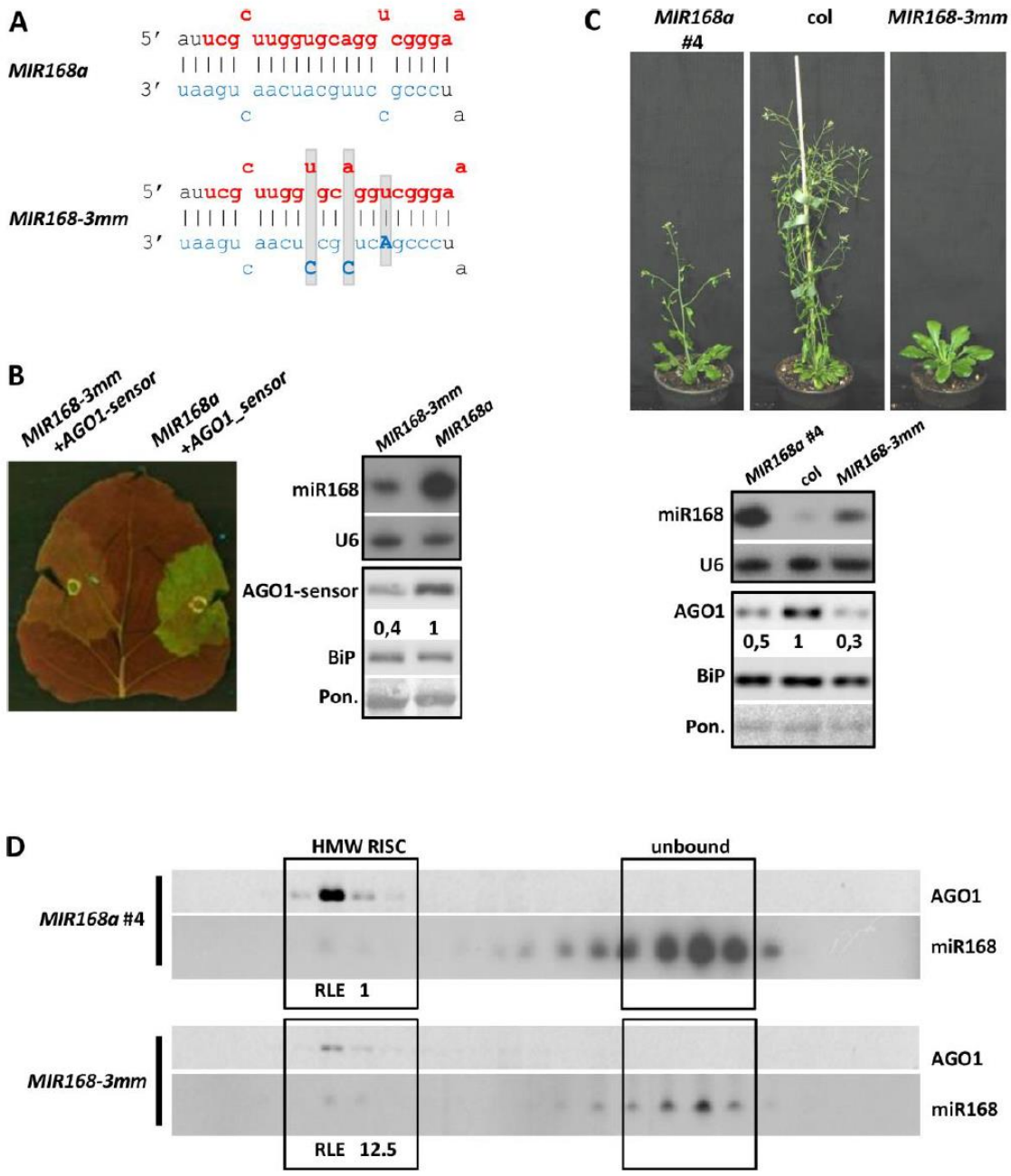

Figure 3. Effect of *MIR168_3mm* over-expression. (A) Structure of the modified duplex region in *MIR168-3mm* in comparison with wild type *MIR168a* duplex. Modified nucleotides of star strand are highlighted with bold capital letters, grey background indicates structural changes. (B) Transient over-expression of *MIR168-3mm* and wild type *ath-pri-MIR168a* (*MIR168a* on figures). Blots demonstrate miR168 and AGO1-sensor content of infiltrated patches of *N. benthamiana* leaves. AGO1 part of the sensor fusion protein was detected with antibody raised against ath-AGO1. For the northern blot U6, while for the western blots, BiP and Ponceau staining were used as loading controls. (C) Phenotype, miR168 and AGO1 content of a transgenic line over-expressing *MIR168-3mm* precursor and a wild type *ath-pri-MIR168a* line with a comparable over-expression rate of miR168. (D) MiR168 distribution in gel-filtration fractions of the investigated lines. High molecular weight (HMW) RISC is represented with AGO1. Relative loading efficiency (RLE) is calculated as described in Methods.

MiR168 produced from *MIR171* based artificial stem-loop structures exhibits increased AGO1 down-regulation capacity

MIR168-3mm construct exhibits *hvu-MIR171* specific features in miR168/miR168* duplex region but the backbone is derived from *MIR168a*. To test further whether the observed differences in loading efficiency are dependent on the precursor RNA sequence or structure we built different artificial miR168 precursor (*AMIR*) constructs based on the modified version of barley *hvu-MIR171* precursor. Three variants of artificial *AMIR* constructs were created to express miR168 from *hvu-MIR171* backbone. To retain the *hvu-MIR171* stem-loop structure we changed the orientation of miR168 guide strand and modified the star strand in order to keep the distribution of the three mismatches within the duplex in the same positions as in hvu-miR171 duplex (Fig. 4A). *AMIR-1* and *AMIR-2* differ only in the identity of mismatched nucleotides in the duplex at 4th and 9th positions. In addition to the changes introduced into *AMIR-1*, *AMIR-3* possesses a G-U base pair in the stem part of the duplex to re-construct the thermodynamic stability of *hvu-MIR171* stem-loop. These miR168 producing *AMIR* precursor constructs (*AMIR-1 -2 -3*) were expressed transiently in *N. benthamiana* leaves by agroinfiltration in the presence of *AGO1-sensor*. All *AMIR* constructs induced the higher reduction of the GFP signal and the *AGO1-sensor* level (Fig. 4B) compared to *MIR168a*. Moreover, as small RNA northern blot results indicate, the increased AGO1 down-regulation in these cases were not associated with drastically enhanced biogenesis of miR168 compared to wild type *MIR168a* (Fig. 4B). Gel-filtration experiments of crude extracts originated from *AMIR-1*, *AMIR-2* and *AMIR-3* agroinfiltrated leaf patches revealed elevated AGO1-RISC loading ability of miR168 in every case. The highest loading efficiency was associated with *AMIR-3*, where passenger strand was modified to mimic better the thermodynamic stability of *hvu-MIR171* duplex. Complete loading of miR159 showed the existence of functional AGO1-RISCs in HMW fractions of leaves expressing *AMIR* constructs. These membranes were also used to detect miR168 star strands using probes specific for every *AMIR* construct. Signals in the low molecular weight, protein unbound fractions indicate that *AMIR* originated miR168 species exist at least partly in duplex form confirming previous results. These data indicate that production of miR168 from alternative stem-loop structures could increase the AGO1-RISC loading efficiency leading to its enhanced biological activity. To further investigate how altered stem-loop structures affect miR168 AGO1-RISC loading efficiency, transgenic plants were generated expressing artificial miR168 precursor constructs. To assess the biological activity of miR168 species expressed from artificial precursors wild type *MIR168a* over-expressing lines producing the similar amount of miR168 were selected. *AMIR-1* and *AMIR-2* display more pronounced phenotypic alterations compared to wild type *MIR168a* over-expressing line exhibiting later emergence of inflorescence, reduced rosette diameter and AGO1 content (Fig. 4C). The severity of phenotypes of the analysed *AMIR-1* and *AMIR-2* lines correlated with the over-produced level of miR168 (data not shown). Phenotypes of transgenic plants expressing extremely high level of miR168 resembled to that of hypomorph *ago1-25* and *ago1-27* mutants. In contrast, the produced 37 *AMIR-3* transgenic lines showed no or only modest miR168 over-expression. Despite our repeated attempts we were not able to identify lines exhibiting higher miR168 over-expression. This observation suggests that high level of *AMIR-3* originated miR168 may have extremely efficient AGO1-RISC loading ability which could be lethal in

transgenic *A. thaliana* lines. This hypothesis is supported by the fact that *AMIR-3* was the most effective construct in transient assay since lower expression rate of miR168 associated with very efficient AGO1 loading. Alternatively, processing of *AMIR-3* could be inefficient in *A. thaliana* producing only weak over-expressor lines. Next, size separation of protein complexes with gel-filtration experiments were performed from seedlings of selected *AMIR-1* and *AMIR-2* transgenic lines and a control *MIR168a* line. Transgenic over-expression of *AMIR-1* and *AMIR-2* constructs resulted in enhanced miR168 accumulation in AGO-RISC containing fractions in spite of the reduced accumulation of AGO1 (Fig. 4D). Immuno-precipitation experiments from seedlings of *AMIR-1* and *AMIR-2* over-expressing lines confirmed that miR168 incorporation into AGO1-RISC is increased in both cases. Analysis of HTS data confirmed that *AMIR* expressing transgenic constructs produce mainly miR168 in correct length and sequence. Moreover, no increase in *AGO1*-derived siRNA content can be detected. Our experiments show that over-expression of miR168 from artificial precursors can influence the efficiency of miR168 loading rate into the AGO1-RISC inducing increased AGO1 down-regulation and phenotypic alterations.

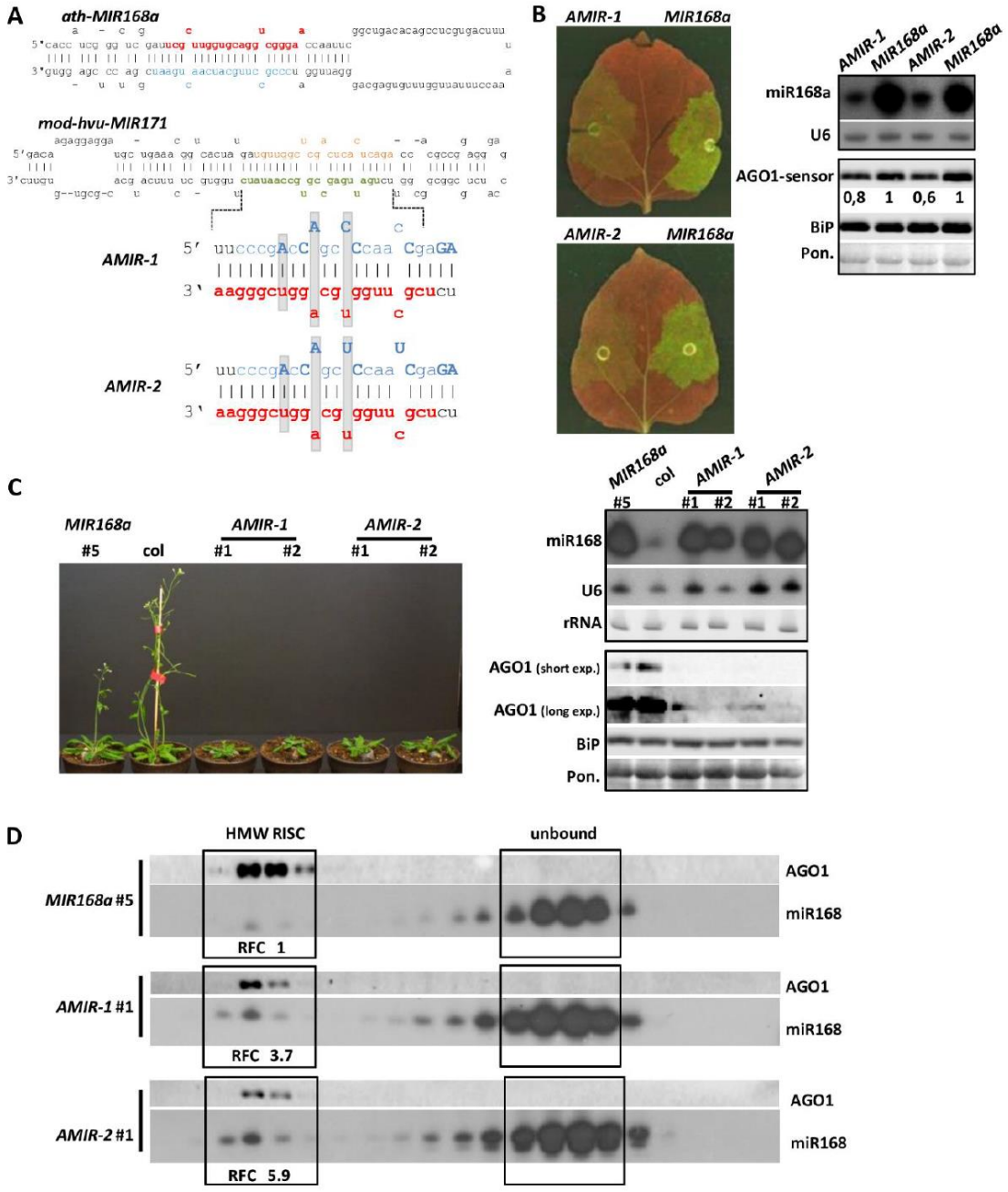

Figure 4. Over-expression of miR168 producing *AMIR* constructs. (A) Structure of the modified duplex region implemented into *hvu-MIR171* backbone in case of *AMIR* constructs. Modified nucleotides of star strands compared to wild type *MIR168a* duplex are highlighted with bold capital letters, grey background show structural changes. (B) Transient over-expression of *AMIR* constructs and wild type *ath-pri-MIR168a* (*MIR168a* on figures). Blots demonstrate miR168 and AGO1-sensor content of infiltrated patches of *N. benthamiana* leaves. AGO1 part of the sensor fusion protein was detected with antibody raised against ath-AGO1. For the northern blot U6, while for the western blots, BiP and Ponceau staining were used as loading controls. (C) Phenotype, miR168 and AGO1 content of transgenic lines over-expressing *AMIR* precursors and a wild type *ath-pri-MIR168a* line with a comparable over-expression rate of miR168. (D) MiR168 distribution in gelfiltration fractions of *MIR168a* #4, *AMIR-1* #1 and *AMIR-2* #1 lines. High molecular weight RISC is represented with AGO1. Relative loading efficiency RLE) is calculated as described in Methods.

Competing miRNAs can affect the loading of miR168 into AGO1-RISC

Our findings show that loading efficiency of miR168 into AGO1-RISC is finely regulated by structural elements of the precursor RNA. This balanced loading efficiency seems to maintain the proper physiological level of AGO1. Modification of the precursor or the secondary structure of the duplex can impair this adjusted loading balance leading to miR168 over/under loading into AGO1-RISC. The general existence of high excess of miR168 pool unbound to AGO1 suggests that the calibrated loading efficiency of miR168 in AGO1-RISC represents a flexible adaptive system. Moreover, this system can be able to rapidly modulate the AGO1 protein content in relation to environmental changes. To test this hypothesis, first we investigated whether loading of miR168 into AGO1-RISC can be competitively altered by modulating the small RNA content of the cellular environment. Previously we demonstrated that in contrast to miR171, miR156 exhibits very inefficient AGO1 loading ability since it accumulates predominantly in protein unbound form in *A. thaliana*. In transient assays, *MIR156* and *MIR171* precursors were massively over-expressed in the presence of *Ago1-sensor* to find out whether the endogenous miR168 can be competitively sequestered from AGO1 loading. We found that robust over-expression of miR171 resulted in a higher GFP signal and slightly increased AGO1-sensor concentration compared to miR156 over-expression (Fig. 5A). This finding indicates that the efficient AGO1 loading of miR171 can inhibit the action of miR168/AGO1 complexes and so the down-regulation of *AGO1-sensor* expression. Size separation gel-filtration assays revealed that the over-expression of well-loading miR171 compared to low-loading miR156 in the agroinfiltrated leaves associated with reduced miR168 content of HMW AGO1-RISC (Fig. 5B). These observations indicate that AGO1 loading of miR168 can respond to alterations in the small RNA pool of the given cellular environment in a competitive manner. To investigate the response of the miR168 loading efficiency based autoregulatory loop to genome wide perturbance in small RNA level *drb1* and *dcl1-9* mutants were analysed. In these mutants the miRNA biogenesis is impaired resulting in decreased level of miRNA pool. Intriguingly, miR168 level was reported to be relatively unaffected in these mutant plants. To maintain the optimal miRNA function and to avoid potential deteriorating effects of the presence of unloaded AGO1-RISCs in these mutants, it is expected that AGO1 protein level is adjusted to the available miRNA pool by the action of miR168/AGO1 regulatory loop. In our experiments, we confirmed that in contrast to miR159, miR168 content was only slightly affected in *drb1* and *dcl1-9* mutants, while AGO1 protein level was remarkably down-regulated (Fig. 5C). Since the low level of AGO1 made technically difficult to use gel-filtration assays immuno-precipitation experiments were carried out. Supporting our hypothesis, the relative miR168 content in AGO1 immuno-precipitates of *drb1* and *dcl1-9* mutants increased (Fig. 5D). These data indicate that in these mutants enhanced miR168 loading into AGO1 forms a new miR168/AGO1 loading equilibrium. This new equilibrium in turn stabilizes a lower AGO1 protein level adjusted to the suppressed miRNA content of the cells.

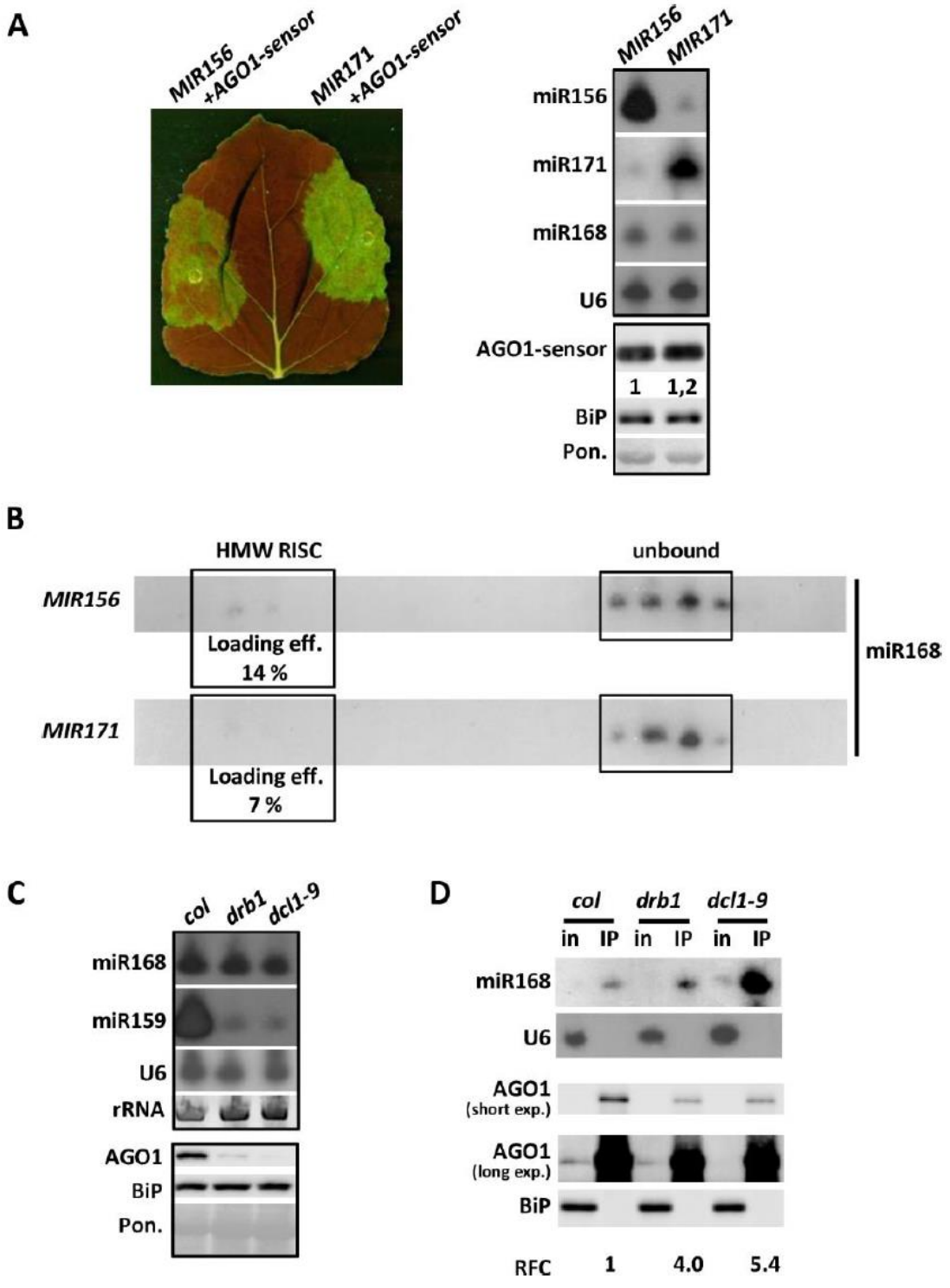

Figure 5. MiR168 loading rate under competitive circumstances. (A) MiR156, miR171, miR168 and AGO1-sensor content of infiltrated patches. U6, BiP and Ponceau staining were used as loading controls of RNA and protein blots, respectively. (B) MiR168 loading in case of *ath-pri-MIR156* or *ath-pri-MIR171* over-expression. Loading efficiency was calculated as the percentage of HMW RISC volume intensity referred to the sum of HMW RISC and unbound volume intensities. (C) MiR168, miR159 and AGO1 in wild type *A. thaliana* Columbia-0 (*col*), *drb1* and *dcl1-9* plants. U6, BiP and Ponceau staining were used as loading controls of RNA and protein blots, respectively. (D) MiR168 accumulation in AGO1 immuno-precipitation samples of *col*, *drb1* and *dcl1-9* plants. Cytoplasmic contamination in IP samples at RNA and protein level was checked with U6 and

BiP, respectively. Relative fold change (RFC) was calculated as the volume intensity ratio of IP and corresponding input samples normalized to AGO1 signal intensity of IP samples, and was represented on the basis of wild type Columbia (*col*).

Based on these data we provide a new model for miR168-AGO1 loading regulation.

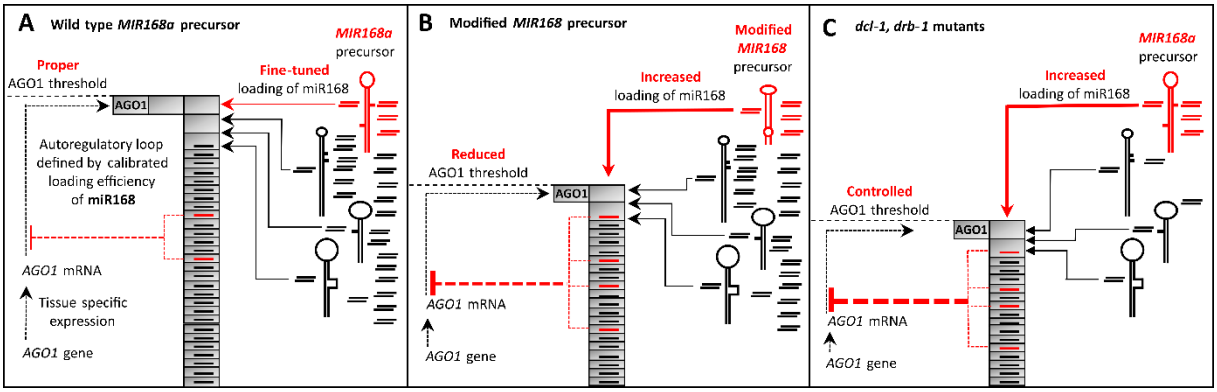

Model for calibrated loading efficiency based miR168-AGO1 autoregulatory loop. (A) Action of *MIR168a* precursor in wild type plant. *AGO1* mRNA, possessing miR168 recognition site, is expressed by tissue specific manner under the control of AGO1 gene promoter (dotted black line with arrowheads). Unloaded AGO1 proteins (gray rectangles) are continuously translated from the mRNA. MiRNA precursors are also expressed in a tissue specific manner (schematically represented by black hairpin structures), including *MIR168a* precursor (red), which are subjected to subsequent cleavages to produce miRNA duplexes (short paired lines) determining the composition of the miRNA pool. The mature miRNA strand of the miRNA duplexes can associate with AGO1 proteins with different efficiencies (lines with arrowheads) generating miRNA loaded AGO1 pool (grey rectangles (AGO1) with lines (miRNAs)). MiRNA duplexes not able to load into AGO1 can accumulate in protein unbound forms (paired lines on the right side of the precursor structures). The AGO1 loading of miR168 is finely calibrated by structural features of the precursor RNA allowing only a subset of the miR168 pool to be loaded into AGO1 (grey rectangles with red line) and majority of miR168 accumulates in duplex form, unbound to protein (red paired lines on the right side of the precursor structures). Due to this highly sensitive autoregulatory loop, the defined miR168/AGO1 complexes negatively regulate *AGO1* mRNA (red dashed lines) determining the proper physiological AGO1 threshold (schematically represented by the column of miRNA loaded AGO1 proteins (gray rectangles with lines). (B) Expression of miR168 from modified precursors, *MIR168-3mm* or *AMIRs*. Modification of the secondary structure of the miR168 producing precursor RNA can perturb the physiological equilibrium of AGO1 level by increasing the loading efficiency of miR168 (thick red line with arrowhead). The higher level of miR168 loaded into AGO1 executor complexes exert increased negative regulation on AGO1 mRNA (thick dashed red line) adjusting a reduced, physiologically unproper, AGO1 equilibrium. (C) Regulatory action of miR168/AGO1 autoregulatory loop in RNAi defective mutants. In *dcl1-9* or *drb1* mutants the production of endogenous miRNAs is strongly inhibited

except the biogenesis of miR168 (represented by the absence of black paired lines). Because of the lack of AGO1-competent miRNAs there is a danger of over-accumulation of unloaded AGO1 proteins leading to interference with proper cell functions. However, in the absence of efficiently AGO1-competent miRNA species the extensively produced miR168 is able to load into AGO1 proteins with higher efficiency imposing strong control on *AGO1* mRNA. Due to this regulatory mechanism, a new, controlled, AGO1 equilibrium is formed in balance with reduced miRNA content of the cell.

There are confirming and control experiments in process and we intend to publish data in the near future.

3. Establishment a gain of function mutant screen for identification influencing the activity of RNA interference.

To identify unknown regulatory components of the RNA interference pathway we started the establishment of a new type of gain-of-function mutant screen which may help to identify factors cannot be revealed by general loss-of-function mutant screens. We down regulated the activity of a stable GFP transgene in Arabidopsis by introducing an amiRGFP precursor construct. The amiRNA/GFP silenced lines were planned to use in generation of liquid cell-culture and was going to *Agrobacterium* transformed with cDNA expressing library. We expected to observe the come-back of GFP signal due to inhibition of RNAi machinery, however because of the auto-fluorescence of the plant tissues it is very difficult to observe the weak GFP signal characteristic to transgenic *Arabidopsis* plants. To resolve this problem in our test-system, we decided to establish a parallel system using neomycin-phosphotransferase gene as target gene in transgenic plants.

We have designed artificial miRNAs (amiRs) to target this gene, and built a construct of kanamycin resistance gene under the control of constitutive 35S promoter. The later construct contains also a separate GFP gene giving opportunity to use it as an inner control, which could be monitored during subsequent transformations, and handling of progeny. Effectiveness of amiRs raised against neomycin-phosphotransferase was tested in transient assay, and all four amiRKm constructs showed proper Km silencing. To exclude the effect of siRNA pathway against transgenes we decided to use *sde1 Arabidopsis* mutants impaired in this process beside wild type plants, and first construct of neomycin-phosphotransferase and GFP reporter gene was transformed into them. F1 was selected based on Km resistance, self-pollinated and homozygous F2 plants were identified according to their neomycin-phosphotransferase and GFP reporter gene expression profile. Two selected amiRKm construct was successfully transformed into this Columbia wild type and *sde1* mutant *Arabidopsis* plants carrying the neomycin-phosphotransferase and GFP reporter gene in homozygous form.

The transgenic plants have further investigated in crosses and at molecular level to select the best performing lines, suitable for the screening experiments. Primary transformant plants with remarkable amiR expression level were tested for kanamycin resistance gene downregulation and the selected plants were self-pollinated. To generate homozygous lines the offspring was checked for transgene expression and plants with the highest amiR level were

selected. To determine the correct experimental conditions, we have to find the lowest kanamycin concentration which is properly selective for the double transformants.

Due to technical sensitivity of the modified c-DNA library-based gain of function mutant screen the experiments are still under construction and optimization.